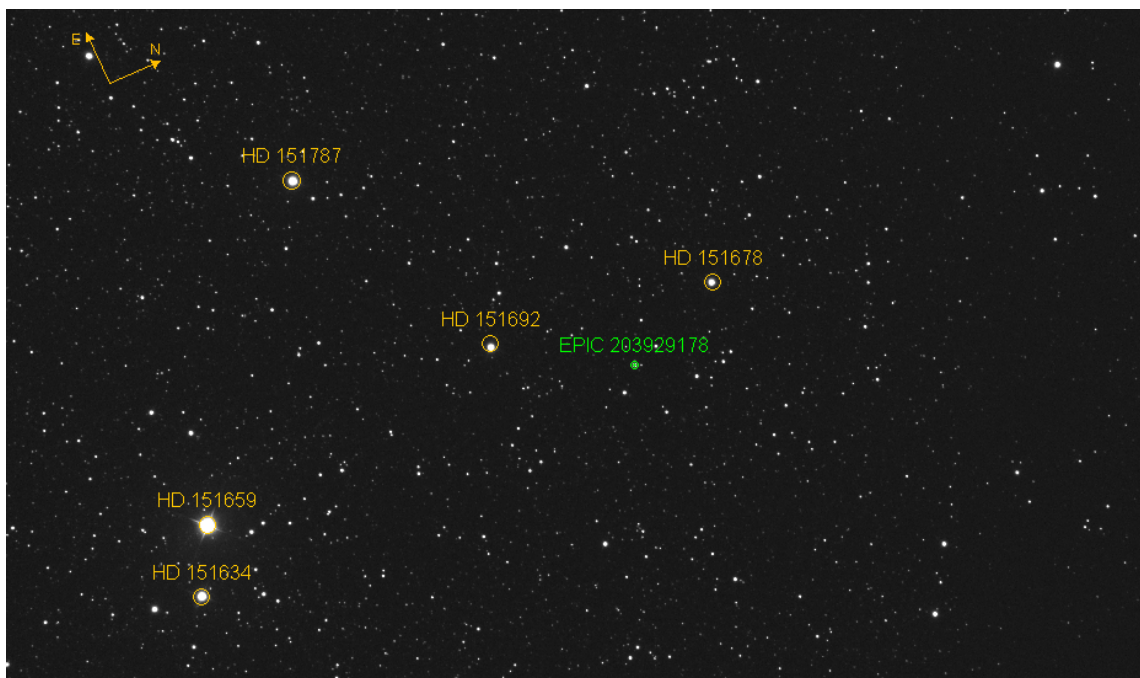# Follow-up studies on exoplanet and eclipsing binary candidates using GoChile

Author: Anže Pirc   Mentor: Jure Japelj

SEPTEMBER 30, 2022

Contents

1 Introduction

The study of exoplanets presents an important subject in understanding how planets form in the universe, letting us then understand their conditions and how they might form life. One way to obtain interesting results is by studying the outliers, the exoplanets with more peculiar characteristics. This was the motivation behind the selection of EPIC 203929178.01. In this report, we will outline the basic concepts in understanding exoplanets, their observation and the results of our research. We will also present the GoChile telescope, the basics of astronomical image calibration and what astronomical parameters are.

An exoplanet is simply any planet outside of our Solar system. The first were discovered in the 1990s[19], after which the numbers of newly detected exoplanets rose rapidly. It is thought that most stars have their own exoplanets and the conditions on them vary considerably. They may be covered in ice, molten rock, have thick atmospheres or none at all, be massive gaseous worlds larger than Jupiter or smaller, rockier planets. And some have may have the right conditions to harbour life, for example planets in the habitable "Goldilocks zone" of stars, where the temperature on the planet is in the range where life can be possible.

Exoplanets can be detected either directly or indirectly. Direct detection through imaging is difficult, since even far away stars seem faint, not to mention their planets. This is why the most popular method of detection, and the one used in this study, is the transit method. As an exoplanet orbits its star, if the system is aligned correctly from our point of view, we can observe the star becoming fainter and brighter as the planet transits in front of it. This change in brightness or flux, can then be measured by telescopes. This method was widely used be the famous Kepler Space Telescope.[26]
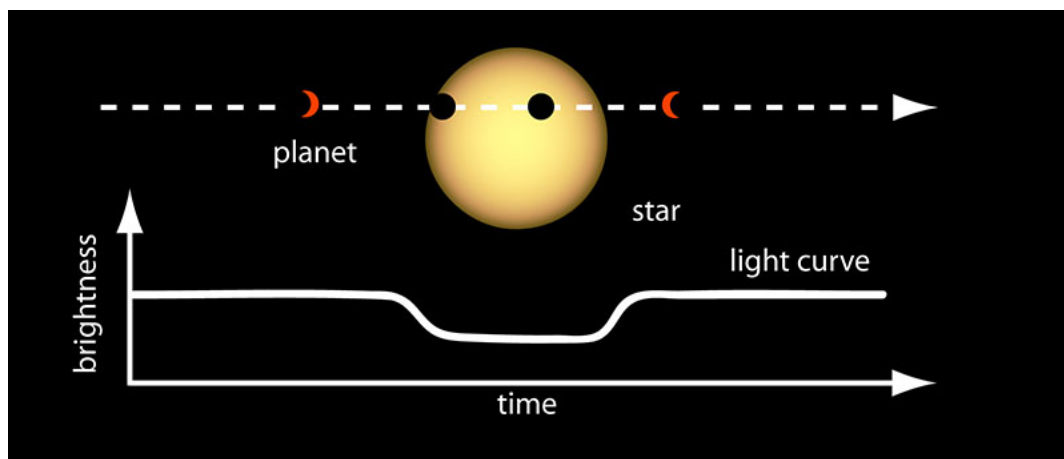

Figure 1: Figure showing a transit of an exoplanet infront of it's star and the corresponding observed lightcurve. This is the basis of the transit detection method. image credit: NASA[12]

Sometimes we see two stars in the sky that appear very close to each other. That could just be because of our line of sight; these are called double stars, like Mizar and Alcor in the Ursa Major constellation. But they are more often than not linked together in other ways; if they are gravitationally bound to each other and orbit each other, they are called binary stars. Sometimes binary stars are positioned in such a way, that we see one star pass in front of the other. These are called eclipsing binaries and can also be detected through the transit method.

The way we can distinguish them from exoplanets is by studying the observed light curve that these stars produce. Instead of one minimum produced by the eclipse, we can observe a smaller, secondary minimum, since the second star also produces light. In general, a binary star light curve looks different from an exoplanet light curve, depending on the size ratio and the distance between the two stars. In some cases, it may look similar and we must then determine the nature of the object by studying the physical parameters.[4]

Exoplanets are usually detected in longer observational campaigns by space-based telescopes and often need to be confirmed by additional observations, especially ones with extreme characteristics.

Our target in this study is EPIC 203929178.01, the name coming from the Ecliptic Plane Input Catalogue. It was discovered as a potential candidate exoplanet by the Kepler K2 campaign[11] in the southern sky, making it observable with GoChile. It lies near the border of the constellations Scorpius and Ophiuchus. Classified as a candidate planet in the NASA Exoplanet Archive[7], this target was chosen owing to its interesting properties. Observations up to this point indicated that it had a considerably large radius of $8.8 \pm 4.6\ R_{Jup}$, making it an unusual size for a planet. This motivated the goal of this paper to try to determine whether EPIC 203929178.01 is in actuality a planet, or a binary star.
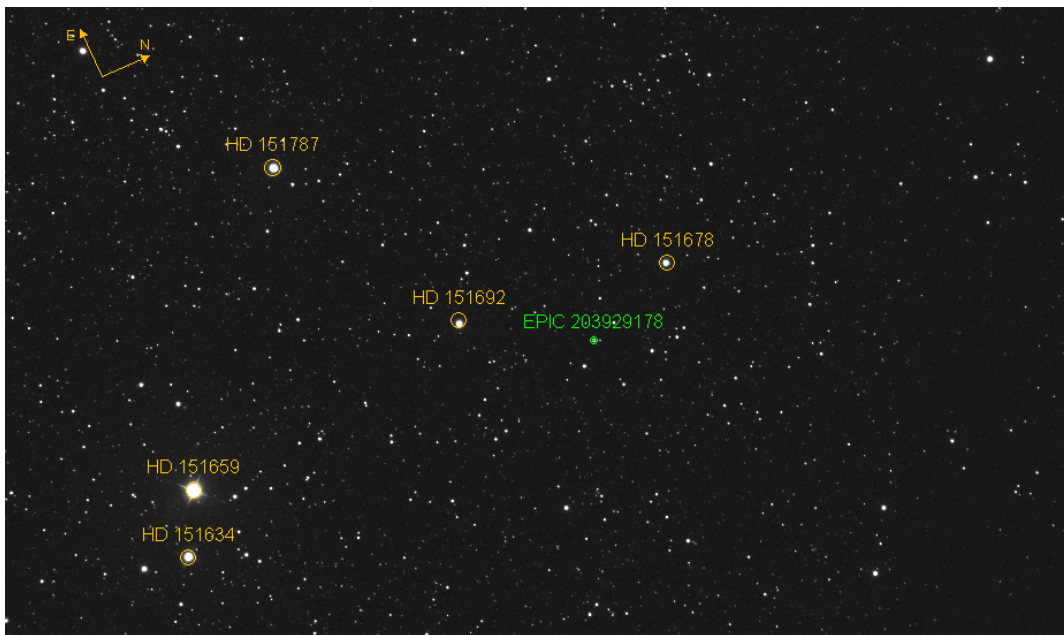

Figure 2: Figure showing the location of EPIC 203929178 and nearby identified stars. The direction in the sky is also shown.

2 Experimental Setup and Observations

Below we present a table detailing all of the attempted and performed observations. They were planned using the Transit Prediction Service provided on the Nasa Exoplanet Archive[17], the STARALT - Object Visibillity website[18] and the Time and Date website[25]. The dates were selected based on when the event was predicted to occur and be most visible e.g. when the Moon was dim, not visible and far away in the sky from our target. Despite this, there were many days when our observations were thwarted by cloudy weather.

Observation date	Filters used	Status
3.5.22	R	Partially Successful
5.6.22	Failed - Bad weather	
6.6.22	L and R	Successful
20.6.22	Failed - Bad weather	
21.6.22	Failed - Bad weather	
5.7.22	L and R	Successful
6.7.22	G and R	Successful
18.7.22	G and R	Successful
19.7.22	G and R	Successful
20.7.22	G and R	Partially successful
21.7.22	G and R	Partially successful
18.8.22	Failed - Bad weather	
19.8.22	G and R	Successful
8.9.22	G and R	Successful
9.9.22	G and R	Successful

Table 1: Table displaying most of the attempted observation dates, filters used and status. The observations from the 10th of September on were all unsuccessful due to bad weather, in total 7 nights of observations.

During the observations, we used atleast two filters each time. This is because different filters pass different amounts of light through them, since the sources do not emit light uniformly. This could also enable us to see (in the case of a binary star) if there are different peaks in different filters, allowing us to possibly seperate the colors of binary stars, since the detectors in the telescope only count how many photons "hit" the detector. In the beginning we used the L or Light filter, which allows all passing photons through. Later this was switched out with the G filter, for more varied information and a lesser risk of oversaturation.

2.1 GoChile

The observations were conducted using the GoChile telescope, run by the University of Nova Gorica and the astronomical magazine Spika[23]. It is located in the south of the Atacama desert in Chile. The exact coordinates of the observatory facility are 30° 27' S and 70° 45' W at 1560 meters above sea level. All the equipment is accessible remotely and is automated, which allows for easier observations, due to the difference in time zones. The telescope has two imaging systems: A smaller 72-mm f/5.6 refractor called GoT2, equipped with an ASI2600MC Pro camera and L, Duo-Band/Ha 656.3 nm and O3 495.9/500.7 nm filters. The larger 400-mm f/6.5 Ritchey-Chrétien called GoT1, was the one used in our observations. It is equiped with an ASI6200MM Pro camera and LRGBHaO3 filters. The telescope is mounted using the ONE50 mount.

Figure 3: Image showing the GoChile telescope pointing at the Chilean sky. Both the imaging systems can be seen. Image credit: Matej Mihelčič

2.2 Software setup

Various programs were used to produce and process the scientific data. AnyDesk[24] was used to connect to the master computer called Vega in Chile. The program called Viking[28] was used to connect to and manage all of the hardware. The main program was Voyager[28], which allowed us to connect several different programs together to automate and perform our observations. The camera was controlled by Maxim DL[16]. After the initial images were obtained, the first step in processing them was to calibrate them using AstroPixelProcessor[3]. After that, the astrometry was performed using the Astrometric Stacking Program or ASTAP[2]. For the photometry, we used AstroImageJ[6] to obtain tabulated raw data and its associated errors. To model the transit of the exoplanet, we used a modified script from the python package PyTransit[20]. This allowed us to extract the astronomical parameters from our data.

3 Data Analysis

3.1 Calibrating Images

The purpose of calibrating scientific images is to increase the signal-to-noise ratio as much as possible in order to improve their quality. One must first then be familiar with the concepts of bias, dark and flat images[22]. A bias image is meant to remove the inherent read-out noise in the camera itself. It is therefore taken with "zero" second exposures, where one obtains an image full of noise, which is later subtracted from the science images. A dark image is meant to reduce thermal noise. This is noise from the ambient temperature around the telescope, which can lead to some pixels in the camera to recieve a signal, even though it is not from light. This is why when taking dark frames, one covers the telescope and exposes the images for preferably the same time as the scientific images, but can also be adjusted, hence the name "dark". These are also then subtracted from the bias-reduced images. Flat frames are used to correct each pixel, so that it gives the same value when exposed to the same amount of light. This allows us to remove motes of dust and lens vignetting present in images. These are taken at dusk or dawn, when the sky is relatively equally illuminated, hence the name "flat". The scientific images are then divided by these.

The actual processing, subtraction and division was done using the program AstroPixelProcessor[3]. After loading all the images, the program procedeed to create the required master frames-combinations of the collected bias, darks and flats, and then applied them to the scientific data.

After image calibration, we needed to perform astrometry on the images. Astrometry measures the exact positions of the stars in the sky using the RA (Right Ascension) and Dec (Declination) coordinates. This was handled in the Astrometric Stacking Program or ASTAP[2]. ASTAP performs astrometry by using a large database of mapped stars. Our images are compared with the ones stored in the database and the exact positions are then calculated and saved in each image. We were then able to connect any pixel in the image to a point in the sky.

3.2 Aperture Photometry

The final step in the image calibration process was to perform aperture photometry. Photometry is the measurement of the intensity of light. Aperture photometry is a technique where the intensity of light (or flux) is measured by selecting a circular aperture around the target star. An inner circle to measure the flux and two outer circles forming an annulus to measure the background flux to subtract from the flux of the star. This was performed using AstroImageJ[6] and it's multiple aperture photometry tool. The name suggests that multiple stars' fluxes are measured to improve the accuracy of the targets flux. This finally gave us the data needed to see our exoplanet transit and plot the light curves we will see in the results section. AstroImageJ calculated the relative flux by comparing multiple reference stars, 12 in our case for each set of data, and also calculated the errors on that relative flux.
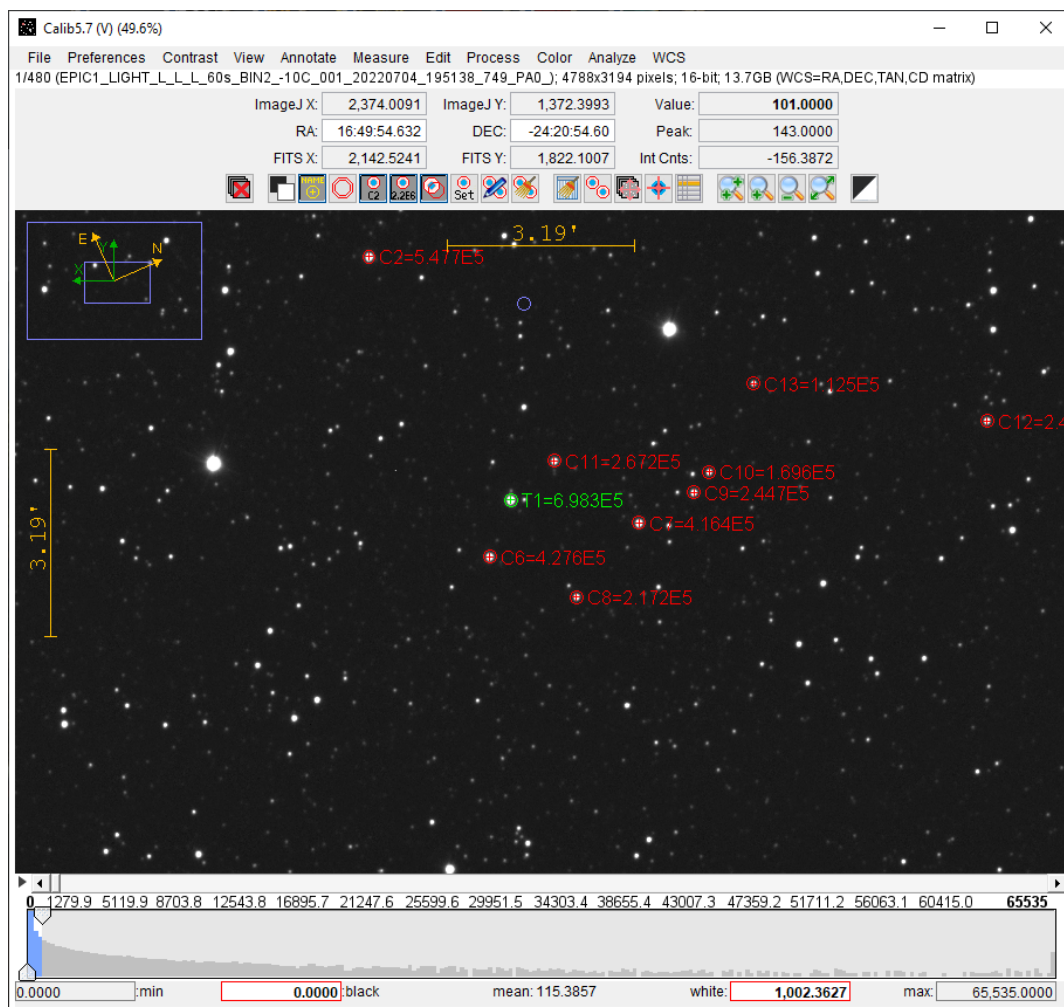

Figure 4: An example of using Multi aperture photometry in AstroImageJ. We see the target star in the green and the reference stars in the red apertures. The more reference stars, the greater the accuracy.

3.3 Light Curve Modelling

Now that we possesed the required datasets, we could begin to extract relevant information from them. For this purpose, we used an exoplanet transit moddeling software called PyTransit[20]. PyTransit is a python package that allowed us to load our light curve data and produce models that were the closest match to the data provided. From those models, we were then able to extract the relevant astronomical parameters, one of the most important being the planet-to-star ratio of radii. Using information collected from various stellar catalogues, we were able to calculate the host stars radius. From this we would finally obtain the important result of the exoplanet radius.

We will explore some basic concepts of exoplanetary transits and the relevant quantities needed for these. The following is largely adapted from P. A. Wilson[1]. One very important quantity is the transit duration T_{dur} itself. To understand it, we must first understand the impact parameter, labeled b. It is the projected distance between the centre of the star and the planet at conjuction, which means when the two bodies are most closely aligned as viewed from Earth. If we assume a circular orbit, the impact paramter is expressed as:
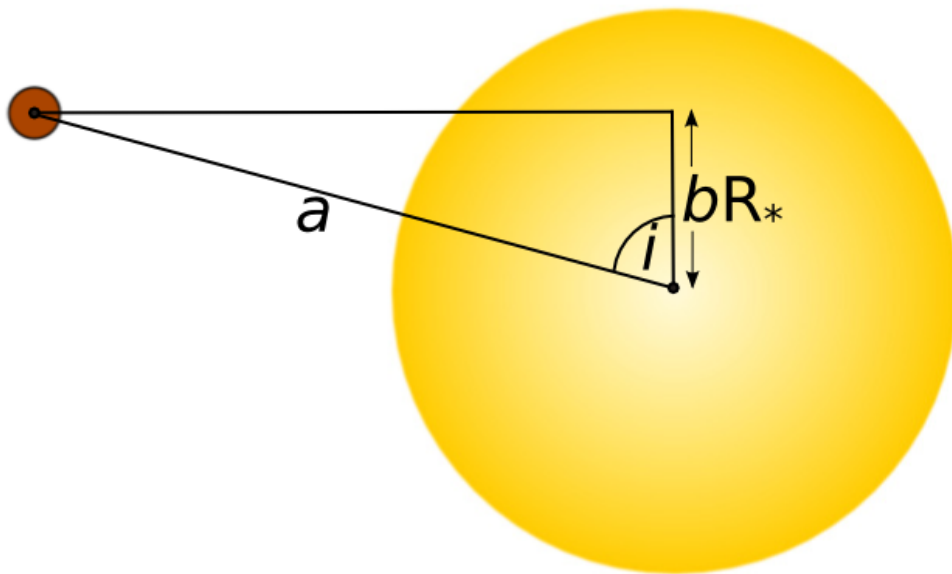
$$b = \frac{a \cos i}{R_*}$$

Figure 5: Figure ilustrating the impact parameter, assuming a circular orbit. Here we can see that it varies from b=0 at the centre of the star to b=1 at the edge. Source[1]

Where i is the inclination, a is the semi-major axis and R_* is the stellar radius.

The total transit duration T_{dur} is defined as the time during which any part of the planet obscures the host star. Using the Pythagorean theorem and the ilustration below, we can express the length that the planet has to travel across the stellar disk as:

$$2l = 2\sqrt{(R_* + R_p)^2 - (bR_*)^2}$$

Figure 6: Figure ilustrating the setup for obtaining the transit duration, assuming a circular orbit. Source[1]

Where R_p is the planetary radius. The full distance travelled is then $2l$. To obtain the transit duration, we then look at the broader orbital geometry.
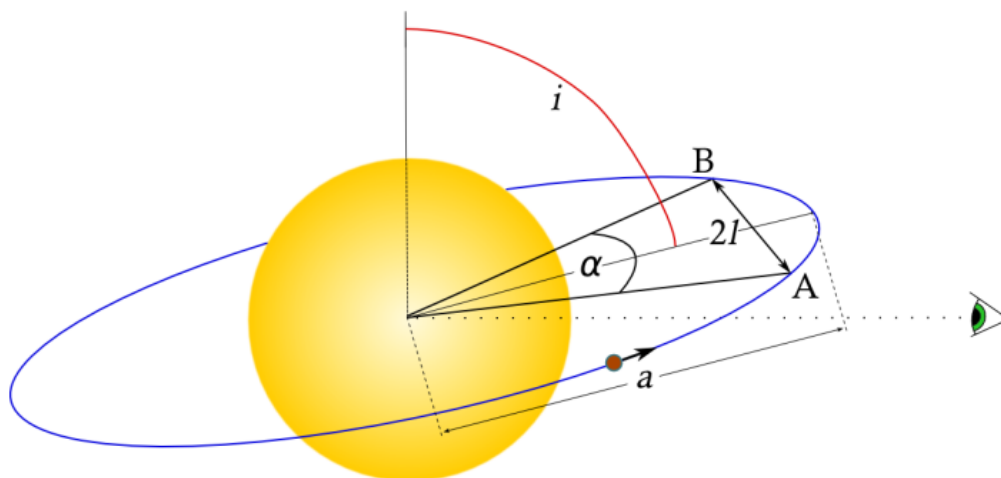

Figure 7: Figure ilustrating the orbital geometry of an exoplanet transit. Source[1]

Because we assume a circular orbit, we can say that the distance around the entire orbit is $2\pi a$, where a is the radius of the orbit, here also the semi-major axis. The arclength between points A and B is then αa. If we divide these two quantites, we get a fraction representing the size of the length between A nd B to the whole orbit. We can multiply this by the orbital period P to obtain T_{dur}:

$$T_{dur} = P \cdot \frac{\alpha}{2\pi} \tag{1}$$

Using the triangle formed by A, B and the centre of the star, we obtain the relation:

$$\sin\frac{\alpha}{2} = \frac{l}{a} \tag{2}$$

which we can then use to obtain an expression for the full transit duration, by combining it with the expression for the length travelled as:

$$T_{dur} = P \cdot \sin^{-1}\left(\frac{l}{a}\right) = \frac{P}{\pi}\sin^{-1}\left(\frac{\sqrt{(R_* + R_p)^2 - (bR_*)^2}}{a}\right) \tag{3}$$

Another important factor for exoplanet transits is the inclination itself. Below we can see how it affects the transit light curve.
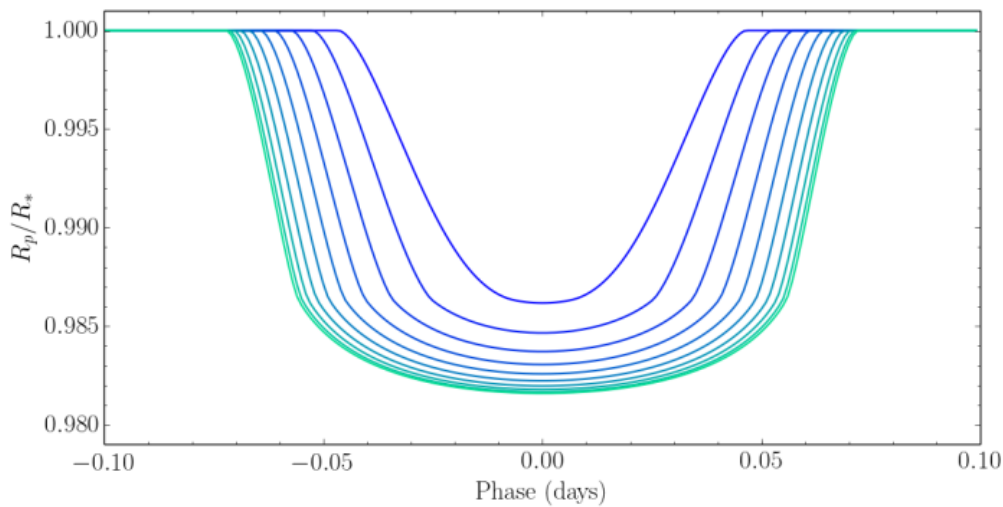

Figure 8: Figure ilustrating how changing the value of the inclination impacts the lightcurve. Here, i ranges from 90° to 80° at 1° intervals. Source[1]

We are now in a better position to understand the following results of our observations and their implications.

4 Results and Discussion

Below we will present our compiled data and results obtained from the various programs used. We begin with an overview of the recorded transits after they have been normalized and fitted using PyTransit.
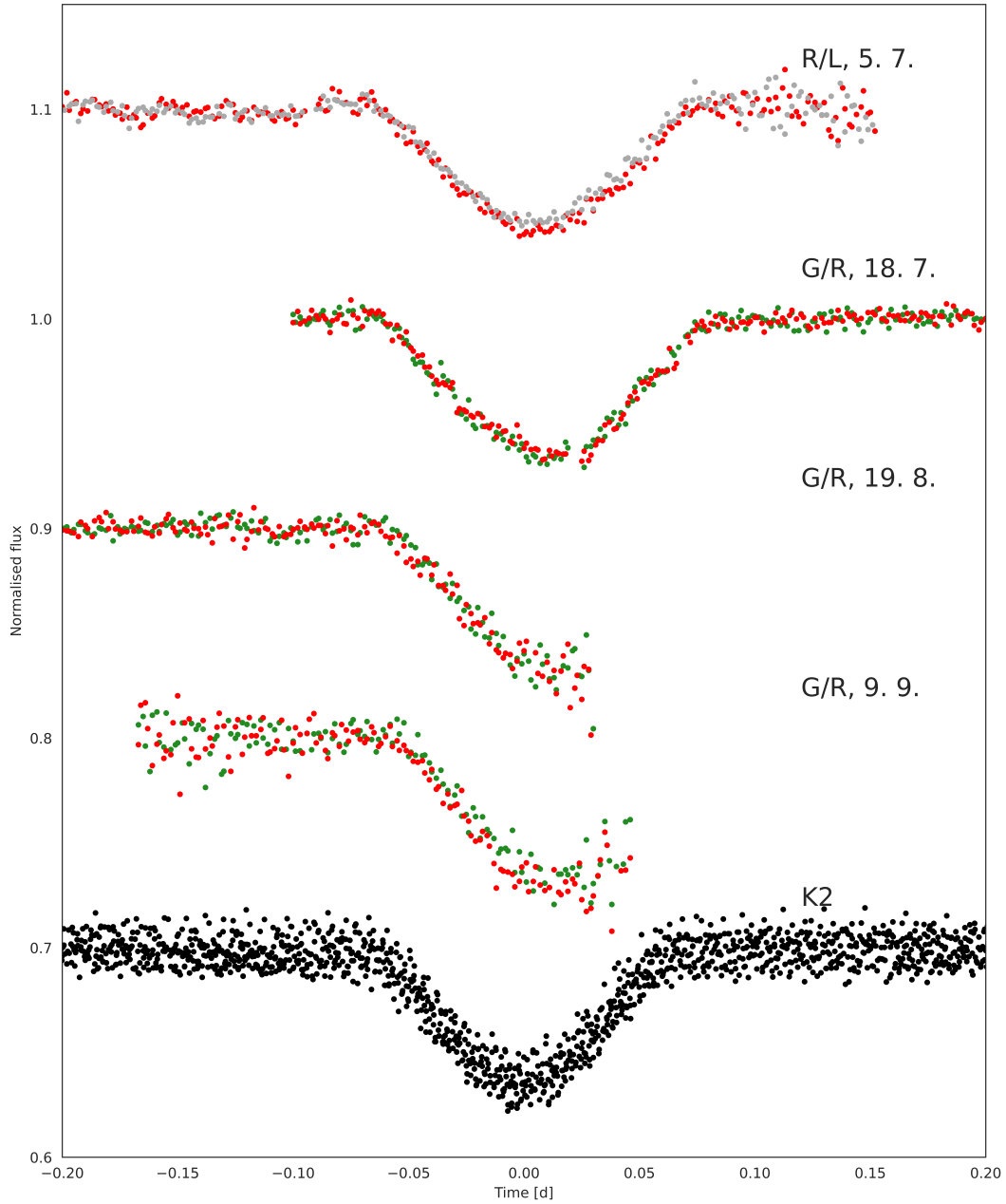

Figure 9: Figure displaying the observed transits. The light flux has been normalized using PyTransit[20]. The minimums were chosen as the zero point on the x-axis and the plots were repositioned accordingly. The last curve in black is data from The Kepler Space Telescopes K2 mission for comparison. The colors of the data points correspond to the respective filters used to record the data.

In order to obtain parameters from these plots, we must first combine them using the same filters to obtain a more complete picture.
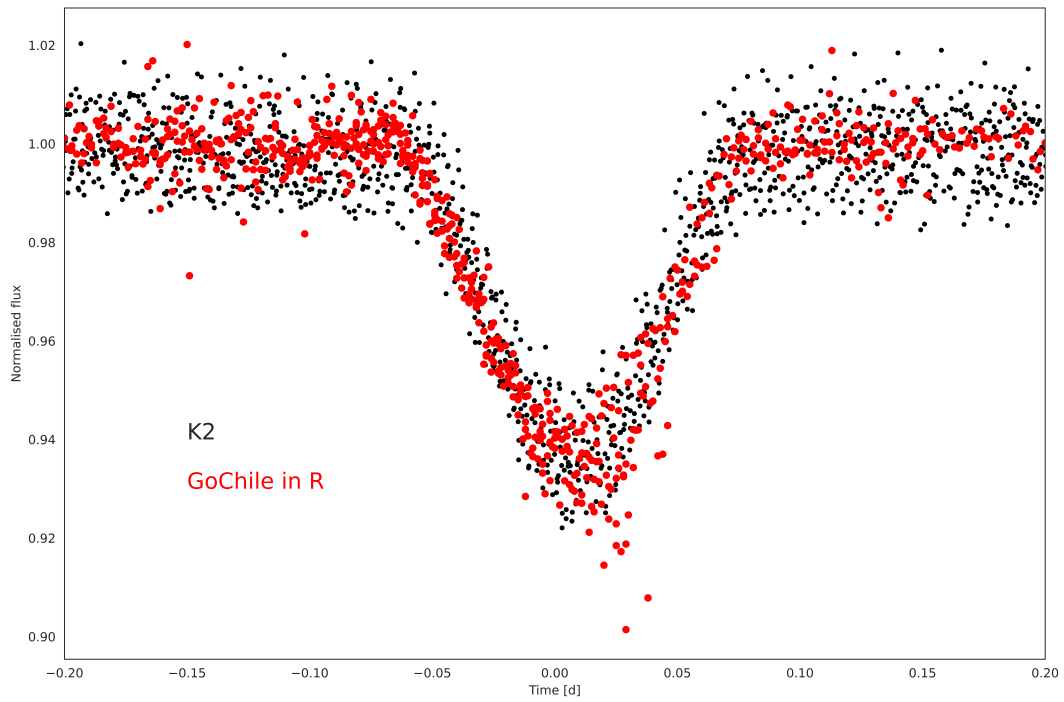
Figure 10: Figure displaying the combined transit data in the R filter with the K2 data for comparison.

PyTransit was then able to obtain the best fitting parameters by exploring the parameter space through an MCMC algorithm.
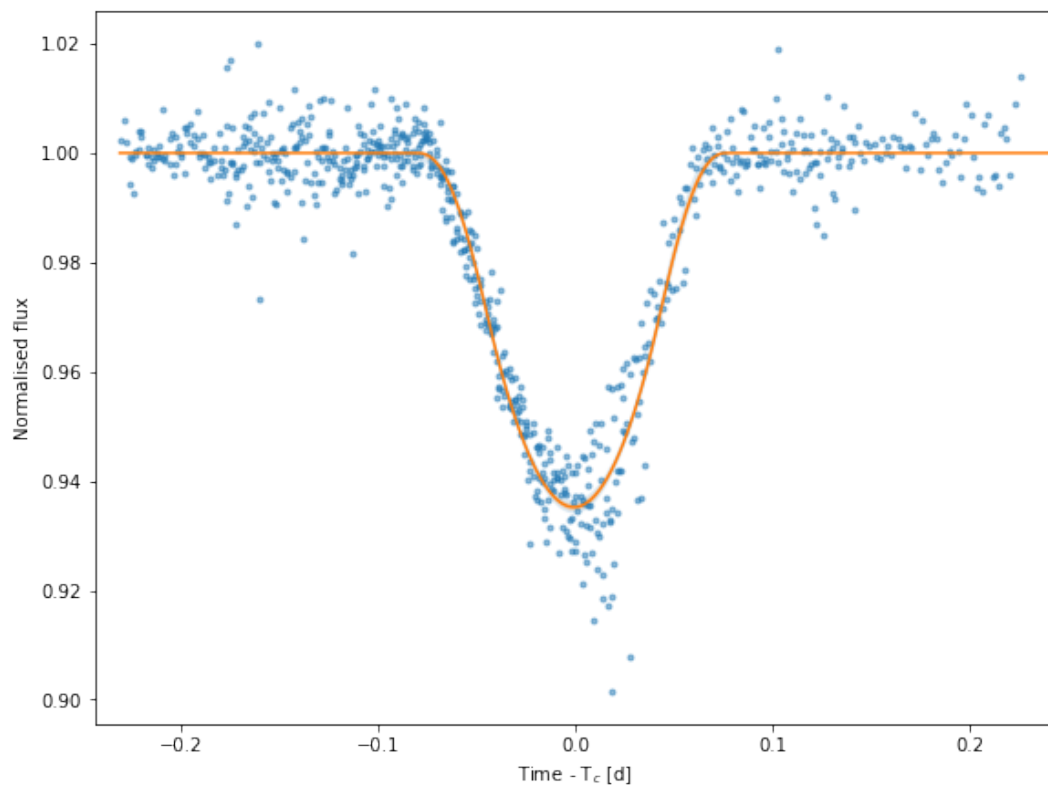

Figure 11: Figure displaying the combined transit data in the R filter with a best fitting curve

We continue with the parameters calculated from the above plots, presented in the following table.

Parameters	Results with $\pm$ 1 sigma equivalent
Planet-star radius ratio	$0.21964^{+0.00294}_{-0.00746}$
Semi-major axis in stellar radii	$2.63463^{+0.18802}_{-0.31580}$
Orbital eccentricity	$0.13559^{+0.29184}_{-0.10962}$
Argument of periastron [rad]	$0.33561^{+0.86250}_{-1.46782}$
Orbital inclination [rad]	$1.34374^{+0.04619}_{-0.20964}$
Transit duration [d]	$0.15174^{+0.00649}_{-0.02254}$
Duration of the "full" transit [d]	$0.07681^{+0.00377}_{-0.01145}$

Table 2: Table showing the calculated astrophysical parameters of EPIC 203929178.01 and their respective 1 sigma errors. A "full" transit is the part of the transit where the exoplanet is not in ingresse or egresse, meaning it is fully inside the stellar disk. Calculated using PyTransit.[20]

4.1 Planet radius

The most relevant piece of information for our purpose is the planet-star radius ratio. From here we can determine the size of the planet if we first know the size of the host star. We can determine its size using its known characteristics from previous catalogues and studies and by using common astrophysical equations.[8] We begin with the equation for the luminosity of a star:

$$L = 4\pi R^2 \sigma T^4 \tag{4}$$

Where L is the luminosity in Watts, R is the radius in meters, σ is the Stefan-Boltzmann constant ($5.67 \cdot 10^8 W m^{-2} K^{-4}$), and T is the star's surface temperature in Kelvin. To obtain the radius, we will divide the above equation with the same one using solar parameters to obtain:

$$\frac{L}{L_S} = \frac{4\pi R^2 \sigma T^4}{4\pi R_S^2 \sigma T_S^4} \tag{5}$$

Where the variables underlined with S refer to solar parameters. Solving for the ratio of radii we get:

$$\frac{R}{R_S} = \left(\frac{L}{L_S}\right)^{\frac{1}{2}} \left(\frac{T}{T_S}\right)^2 \tag{6}$$

To solve for the ratio of luminosities, we will use Pogsons formula:

$$\frac{L}{L_S} = 10^{0.4 \cdot (m_S - m)} \tag{7}$$

13

Where m is the apparent magnitude and m_S the apparent magnitude of the sun. These two magnitudes may be replaced by their respective absolute magnitudes. To find them we begin with looking up the host star in SIMBAD[27]. From there we obtain data about its visual apparent magnitue[10] of $m_V = 11.34 \pm 0.17$ and the stars parallax[9] of $p = 1.4776 \pm 0.1882$ mas. Since the apparent magnitude is given in the visual spectrum, when converting to the absolute magnitude, we will need to use the bolometric correction in order to obtain the bolometric absolute magnitude. Bolometric means that this magnitude takes into account all wavelengths of light. To find the absolute magnitude, we use:

$$M = m - 5 \cdot \log_{10}(d_{pc}) + 5 \tag{8}$$

Where d_{pc} is the distance to the star in parsecs. We can obtain this by: $d_{pc} = \frac{1}{p}$, where p is the parallax measured in arc-seconds. Combining the cited parallax and magnitude, we obtain $d_{pc} = 676.77 \pm 0.09 pc$ and therefore $M_V = 2.19 \pm 0.17$, where V denotes that the absolute magnitude applies to the visual part of the light spectrum. This is why we must now use the bolometric correction in order to obtain the bolometric absolute magnitude as:

$$M_{bol} = BC + M_V \tag{9}$$

Where BC is the bolometric correction. We obtain this correction with the help of the effective surface temperature of the star $T_{eff} = 6820 \pm 64 K$[29]. At this temperature, the bolometric correction is BC=-0.005[13], giving us an absolute bolometric magnitude of $M_{bol} = 2.1828 \pm 0.17$. The absolute bolometric magnitude of the sun is $M_{S-bol} = 4.74 \pm 0.0004$[21].This allows us to obtain the ratio of luminosities as: $\frac{L}{L_S} = 10^{0.4 \cdot (2.5572)}$. We now also need the solar effective temperature $T_S = 5772 \pm 0.8 K$[21]. We can now finally obtain the stellar ratio as:

$$\frac{R}{R_S} = \left(10^{0.4 \cdot (2.56 \pm 0.17)}\right)^{\frac{1}{2}} \left(\frac{6820 \pm 64 \text{ K}}{5772 \pm 0.8 \text{ K}}\right)^2 = 2.3257 \pm 0.0805 \tag{10}$$

This gives us a stellar radius of R=2.3257 R_S in units of solar radii. From this we can use the earlier planet-star ratio of radii to obtain our final result for the exoplanet radius as:

$$R_p = 0.5108^{+0.0190}_{-0.0248} \, R_S \tag{11}$$

Due to the very large radius leads us to conclude that this may not be an exoplanet at all, but a companion star in a binary system. We can take a look at Jingjing and Kipping 2017.[5]

To propagate and obtain all the previous errors, we used the general formula for error propagation at each step of calculating a new variable. The equation is defined as:

$$\sigma_x^2 = \left(\frac{\partial x}{\partial a}\right)^2 \sigma_a^2 + \left(\frac{\partial x}{\partial b}\right)^2 \sigma_b^2 + \left(\frac{\partial x}{\partial c}\right)^2 \sigma_c^2 \tag{12}$$

where σ_x is uncertainty on the variable x, while a,b and c are variables with their own uncertainties composing the function x.
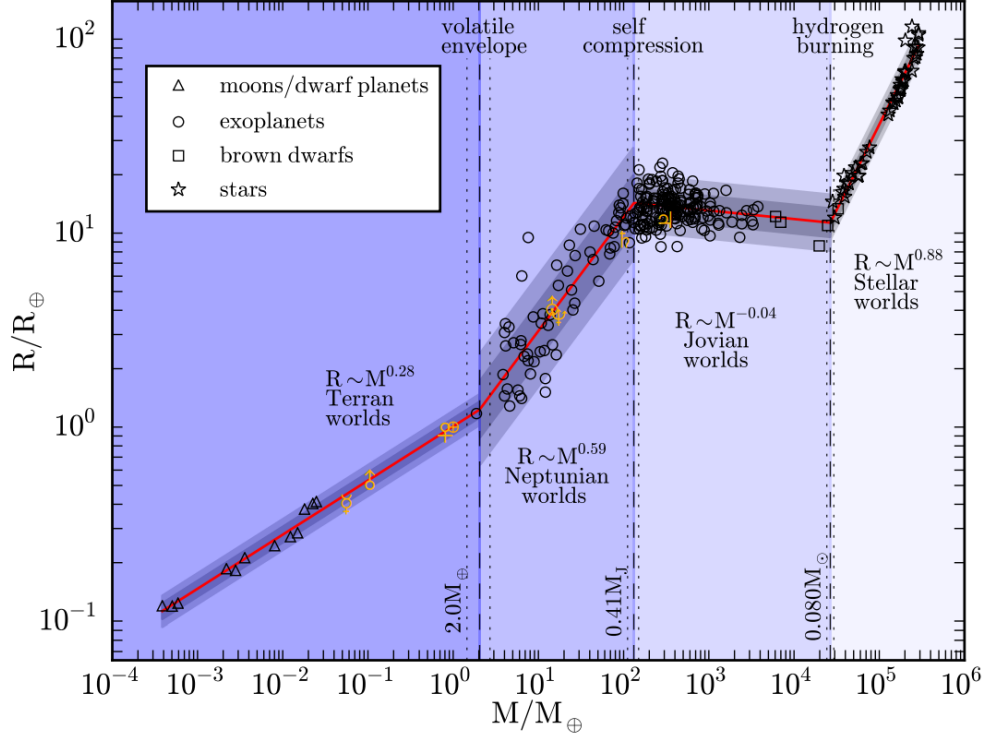
Figure 12: The mass-radius relation from dwarf planets to late-type stars from Jingjing and Kipping 2017. Points represent the 316 data against which their model is conditioned, with the data key in the top-left. Although the error bars weren't plotted, both radius and mass uncertainties are accounted for. The red line shows the mean of the probabilistic model and the surrounding light and dark gray regions represent the associated 68% and 95% confidence intervals, respectively. The plotted model corresponds to the spatial median of their hyper parameter posterior samples.[5]

In the third figure from the paper, seen above, we can see that our target is most likely a star, since the limit for exoplanets is roughly around 2 Jupiter radii (or around 22 Earth radii). Our target has a radius of R=55.74 R_{Earth} indicating that it is in the hydrogen fusing region of the graph and most likely a star.

4.2   Non-detection of the secondary minimum

Since we see that the target is most likely a star, we must note the lack of a secondary minimum. We can explain this by comparing the luminosities of both stars using the mass-radius relation and mass-luminosity relation. Assuming the two stars are main-sequence stars, we can roughly obtain their masses by[15]:

$$\log R = 0.003 + 0.724 \log M \tag{13}$$

This gives us the mass of the primary as $M_{pri} = 3.2$ and the mass of the secondary star(our traget) as $M_{sec} = 0.4$. From here, we can then use the mass-luminosity relation given as[14]:

$$\frac{L_{sec}}{L_{pri}} = \left(\frac{M_{sec}}{M_{pri}} \right)^{3.5} \tag{14}$$

This in turn gives us a luminosity ratio of $\frac{L_{sec}}{L_{pri}}$=0.0007. This tells us that the secondary star has much lower luminosity than the primary, according to equation 7, this gives us a difference in magnitude of around 8. This is much lower than the resolution of GoChile and would explain the apparent lack of a secondary minimum.

5 Conclusion

In this work we have concluded that the candidate exoplanet EPIC 203929178.01 is most likely a companion star in a binary system. This was motivated by its more remarkable characteristics listed in the NASA Exoplanet Archive[7]. We obtained our main result of the targets radius of $R_t = 0.5108 R_S$ and determined from Jingjing and Kipping[5] that this is too large of a radius to still be considered a planet. We however did not observe the characteristic secondary minimum of binary star systems in our observations, because GoChile is not a powerfull enough telescope to resolve such a large difference in magnitude. To better improve the accuracy of our measurements and calculations in the future and add more weight to our conclusion, we suggest that a higher amount of observations be taken in longer interval for more data, as we had limited data due to frequent problems with bad weather. Another suggestion is to use a more detailed analysis where we take the colour filters into account, along with a more powerfull telescope to possibly observe the secondary minimum.

References

[1] Paul A. Wilson. *The Exoplanet Transit Method*. Eng. URL: https : / / www . paulanthonywilson . com / exoplanets / exoplanet - detection - techniques / the-exoplanet-transit-method/.

[2] *ASTAP, Astrometric Stacking Program*. URL: https://www.hnsky.org/astap.htm#index (visited on 09/27/2022).

[3] *Astro Pixel Processor*. en-US. URL: https : / / www . astropixelprocessor . com/ (visited on 09/27/2022).

[4] *Binary Stars*. URL: http : / / abyss . uoregon . edu / ~js / ast122 / lectures / lec10.html (visited on 09/25/2022).

[5] Jingjing Chen and David Kipping. "Probabilistic Forecasting of the Masses and Radii of Other Worlds". In: *The Astrophysical Journal* 834 (Jan. 2017). ADS Bibcode: 2017ApJ...834...17C, p. 17. ISSN: 0004-637X. DOI: 10 . 3847 / 1538 - 4357 / 834/1/17. URL: https : / / ui . adsabs . harvard . edu / abs / 2017ApJ . . . 834 . . . 17C (visited on 09/28/2022).

[6] Karen A. Collins et al. "ASTROIMAGEJ: IMAGE PROCESSING AND PHOTOMETRIC EXTRACTION FOR ULTRA-PRECISE ASTRONOMICAL LIGHT CURVES". In: *The Astronomical Journal* 153.2 (Jan. 2017), p. 77. ISSN: 1538-3881. DOI: 10 . 3847 / 1538 - 3881 / 153/2/77. URL: https://iopscience.iop.org/article/10.3847/1538-3881/153/2/77 (visited on 09/27/2022).

[7] *EPIC 203929178 | NASA Exoplanet Archive*. URL: https : / / exoplanetarchive . ipac . caltech . edu / overview / EPIC % 20203929178 . 01 # planet _ EPIC - 203929178 - 01 _ collapsible (visited on 09/27/2022).

[8] *Finding the Radius of a Star*. URL: https : / / cas . sdss . org / dr4 / en / proj / advanced/hr/radius1.asp (visited on 09/25/2022).

[9] Gaia Collaboration. "VizieR Online Data Catalog: Gaia EDR3 (Gaia Collaboration, 2020)". In: *VizieR Online Data Catalog* (Nov. 2020). ADS Bibcode: 2020yCat.1350....0G, pp. I/350. URL: https://ui.adsabs.harvard.edu/abs/2020yCat.1350....0G (visited on 09/28/2022).

[10] E. Høg et al. "The Tycho-2 catalogue of the 2.5 million brightest stars". en. In: *Astronomy and Astrophysics* 355 (Mar. 2000), pp. L27–L30. ISSN: 0004-6361. URL: https://ui.adsabs.harvard.edu/abs/2000A&A...355L..27H/abstract (visited on 09/28/2022).

[11] Michele Johnson. *A Spacecraft's Second Life: NASA's K2 Mission*. und. Text. Mar. 2016. URL: http : / / www . nasa . gov / feature / ames / nasas - k2 - mission - the - kepler - space - telescopes - second - chance - to - shine (visited on 09/27/2022).

[12] *Light Curve of a Planet Transiting Its Star*. URL: https : / / exoplanets . nasa . gov / resources / 280 / light - curve - of - a - planet - transiting - its - star (visited on 09/29/2022).

[13] Eric Mamajek. *"A Modern Mean Dwarf Stellar Color and Effective Temperature Sequence"*. Apr. 2022. URL: https : / / www . pas . rochester . edu / ~emamajek / EEM_ dwarf_UBVIJHK_colors_Teff.txt.

[14] *mass-luminosity relation*. URL: http : / / astro . vaporia . com / start / massluminosity . html (visited on 09/30/2022).

[15] *mass-radius relation*. URL: http://astro.vaporia.com/start/massradius.html (visited on 09/30/2022).

[16] *MaxIm DL - Astronomy & Scientific Imaging Solutions*. en-US. URL: https : / / diffractionlimited . com / product / maxim-dl/ (visited on 09/27/2022).

[17] *NASA Exoplanet Archive: Transit Service.* URL: https://exoplanetarchive.ipac.caltech.edu/cgi-bin/TransitView/nph-visibletbls?dataset=transits (visited on 09/27/2022).

[18] *Object Visibility.* URL: http://catserver.ing.iac.es/staralt/ (visited on 09/27/2022).

[19] *Overview | What is an Exoplanet?* URL: https://exoplanets.nasa.gov/what-is-an-exoplanet/overview (visited on 09/25/2022).

[20] Hannu Parviainen. "PYTRANSIT: fast and easy exoplanet transit modelling in PYTHON". In: *Monthly Notices of the Royal Astronomical Society* 450 (July 2015). ADS Bibcode: 2015MNRAS.450.3233P, pp. 3233–3238. ISSN: 0035-8711. DOI: 10.1093/mnras/stv894. URL: https://ui.adsabs.harvard.edu/abs/2015MNRAS.450.3233P (visited on 09/27/2022).

[21] Andrej Prša et al. "Nominal Values for Selected Solar and Planetary Quantities: IAU 2015 Resolution B3". In: *The Astronomical Journal* 152 (Aug. 2016). ADS Bibcode: 2016AJ....152...41P, p. 41. ISSN: 0004-6256. DOI: 10.3847/0004-6256/152/2/41. URL: https://ui.adsabs.harvard.edu/abs/2016AJ....152...41P (visited on 09/28/2022).

[22] Practical Astrophotography Staff. *A Brief Guide to Calibration Frames: Bias, Dark, Flats and Dark Flats.* English. June 2018. URL: https://practicalastrophotography.com/a-brief-guide-to-calibration-frames/.

[23] *Teleskop in oprema – GoChile.* sl-SI. URL: https://gochile.si/teleskop-in-oprema/ (visited on 09/25/2022).

[24] *The Fast Remote Desktop Application.* en. URL: https://anydesk.com/en (visited on 09/27/2022).

[25] *timeanddate.com.* en. URL: https://www.timeanddate.com/ (visited on 09/27/2022).

[26] *Transit Method | Institute for Research on Exoplanets.* en-US. URL: http://www.exoplanetes.umontreal.ca/transit-method/?lang=en (visited on 09/27/2022).

[27] *TYC 6809-703-1.* URL: https://simbad.unistra.fr/simbad/sim-id (visited on 09/28/2022).

[28] *Voyager – Astrophotography Automation Software.* en-US. URL: https://software.starkeeper.it/ (visited on 09/27/2022).

[29] Robert A. Wittenmyer et al. "The K2-HERMES Survey. I. Planet-candidate Properties from K2 Campaigns 1–3". In: *The Astronomical Journal* 155.2 (Jan. 2018), p. 84. ISSN: 1538-3881. DOI: 10.3847/1538-3881/aaa3e4. URL: https://iopscience.iop.org/article/10.3847/1538-3881/aaa3e4 (visited on 09/25/2022).